JOURNAL OF CATALYSIS 67, 175–185 (1981)

Evidence for H_2/D_2 Isotope Effects on Fischer–Tropsch Synthesis over Supported Ruthenium Catalysts

C. STEPHEN KELLNER AND ALEXIS T. BELL

Materials and Molecular Research Division, Lawrence Berkeley Laboratory, and Department of Chemical Engineering, University of California, Berkeley, California 94720

Received April 16, 1980; revised August 11, 1980

The effects of using D_2 rather than H_2 during Fischer–Tropsch synthesis were investigated using alumina- and silica-supported Ru catalysts. For the alumina-supported catalysts, the rate of CD_4 formation was 1.4 to 1.6 times faster than the formation of CH_4. A noticeable isotope effect was also observed for higher molecular weight products. The magnitude of the isotope effects observed using the silica-supported catalyst was much smaller than that found using the alumina-supported catalysts. The formation of olefins relative to paraffins was found to be higher when H_2 rather than D_2 was used, independent of the catalyst support. The observed isotope effects are explained in terms of a mechanism for CO hydrogenation and are shown to arise from a complex combination of the kinetic and equilibrium isotope effects associated with elementary processes occurring on the catalyst surface.

INTRODUCTION

Results from a number of recent studies (*1–13*) suggest that the catalytic synthesis of CH_4 from CO and H_2 over group VIII metals proceeds via stepwise hydrogenation of atomic carbon, formed upon dissociation of chemisorbed CO. It has also been proposed that the formation of higher molecular weight hydrocarbons is initiated by the addition of a methyl group to a methylene group and that further chain growth occurs by the reaction of methylene groups with adsorbed alkyl groups (*14, 15*). The alkyl groups then react to form olefins and paraffins via either hydrogen elimination or addition. Consistent with these views of CO hydrogenation, one would expect to observe an isotopic effect if D_2 were used instead of H_2. While several attempts have been made to observe such an effect, the results available thus far have been contradictory. In early studies by Jungers *et al.* (*16, 17*), the hydrogenation of CO to CH_4 over Ni was observed to proceed more rapidly with D_2 than H_2 and the activation energy was lower for D_2. Recent studies by Mori *et al.* (*18*) have confirmed this observation and indicate that methanation over Ni is 1.4 times faster with D_2 than with H_2. Sakharov and Dokukina (*19*) also observed an inverse isotope effect for a Co/ThO_2/Kieselguhr catalyst. For temperatures between 449 and 466 K they found that the formation of CD_4 was 1.2 to 1.5 times faster than the formation of CH_4. A normal isotope effect was observed by McKee (*20*) for CH_4 synthesis over Ru powder. The ratio of CH_4 to CD_4 formation was 2.2 over the temperature range of 298 to 423 K. In contrast to these results, Dalla Betta and Shelef (*21, 22*) reported that no isotopic effect could be discerned for either CH_4 or total hydrocarbon formation over Ni/ZrO_2, Ru/Al_2O_3, or Pt/Al_2O_3 for temperatures between 423 and 498 K. Based on this evidence it was suggested that CO dissociation is likely to be the rate-determining step in CO hydrogenation. In a comment on these results, Wilson (*23*) noted that the overall isotope effect could arise from a combination of kinetic and equilibrium isotope effects, the former favoring the reaction of H_2 and the latter favoring the reaction of D_2. As a result of this, he concluded that the presence or

0021-9517/81/010175-11$02.00/0

absence of an isotope effect cannot be used to identify the rate-determining step.

The present study was undertaken to reexamine the nature of the H_2/D_2 isotope effect associated with the synthesis of CH_4 and higher molecular weight hydrocarbons over silica- and alumina-supported Ru. These investigations were carried out at 1 and 10 atm in the temperature interval of 453 to 548 K. An inverse isotope effect was observed for the alumina-supported catalysts, which was largest for CH_4 and declined with increasing carbon number. The magnitude of the inverse isotope effect observed using the silica-supported catalyst was much smaller, and a normal isotope effect was observed for some of the products. A small normal isotope effect on the olefin to paraffin ratio was observed over both catalysts. The significance of these observations is discussed in the light of a proposed mechanism for the hydrogenation of CO over Ru.

EXPERIMENTAL

Catalysts. Two alumina-supported catalysts and one silica-supported catalyst were prepared using Kaiser KA-201 γ-alumina and Davidson 70 silica gel as the supports. A 3.0% Ru/Al_2O_3 and a 1.2% $Ru/Si0_2$ catalyst were prepared by incipient wetness impregnation of the support with an aqueous solution of $RuCl_3$, acidified to pH 2 to suppress hydrolysis. The resulting slurry was air dried, and then heated slowly in vacuum from 298 to 423 K. Reduction of the chloride was carried out in flowing H_2. The temperature was raised slowly from 298 to 673 K and then maintained at 673 K for 8 hr.

A second alumina-supported catalyst was prepared by adsorption of $Ru_6C(CO)_{17}$ from a pentane solution under oxygen and moisture-free conditions. Synthesis of the cluster complex and details of the impregnation procedure have been described previously (*24*). Once dried this catalyst, designated as 1.0% Ru_6/Al_2O_3, was reduced in flowing H_2 under conditions identical to those used to reduce the catalysts prepared from $RuCl_3$.

The dispersions of the 1.0% Ru_6/Al_2O_3 and the 3.0% Ru/Al_2O_3 catalysts, measured by H_2 chemisorption, were found to be 1.0 and 0.5, respectively. The dispersion of the 1.2% Ru/SiO_2 catalyst could not be determined by this technique since a reproducible determination of H_2 uptake could not be obtained. As a result, the dispersion of this catalyst was measured by CO chemisorption and determined to be 0.25, based on the assumption that the ratio of CO to surface Ru atoms is unity. The validity of this assumption is supported by previous studies with low dispersion Ru/Al_2O_3 catalysts (*25*) and by the observation that infrared spectra of CO adsorbed on the Ru/SiO_2 used in this study (*7*, *26*) show only a single band, attributable to linearly adsorbed CO.

All reactions were carried using a premixed feed composed of H_2 or D_2 and CO at a ratio of $H_2(D_2)/CO = 3.0$. The feed mixtures were blended in small cylinders using pure components. Following filling, the bottom of the cylinder containing the mixture was heated for 1 day to assure uniform gas mixing. The blended mixture was then analyzed by gas chromatography to establish the concentration of CO. If the original mixture was not correct, additional CO or H_2 (D_2) was added. By following this procedure, it was possible to obtain mixtures containing 25 $\pm$ 0.5% CO.

Procedure. Rate data were obtained using a stainless-steel microreactor heated in a fluidized bed. The reaction products were analyzed using an on-line gas chromatograph fitted with balanced 2.4 mm by 1 m columns packed with Chromsorb 106. The column oven was temperature programmed from 318 to 503 K at 10 K/min, and the hydrocarbon products were detected by a flame ionization detector. Calibration of the chromatograph was carried out using mixtures containing known concentrations of the products. In addition, by injecting pure samples of CH_4 and CD_4 it was established that the detector sensitivities for deuter-

ated and hydrogenated products were identical.

Each experiment with a fresh catalyst charge [30 mg for the 3.0% Ru/Al_2O_3 catalyst and 100 mg for the 1.0% Ru_6/Al_2O_3 and the 1.2% Ru/SiO_2 catalysts] was initiated by a 10 to 12 hr reduction in flowing H_2 at 673 K and 10 atm. The temperature was then lowered to 498 K and the feed mixture was introduced at a flow rate of 200 cm³/min (STP). Ten minutes after the reaction began, a gas sample was taken for analysis and the gas feed was switched over to pure H_2 for 1 hr. By alternating short reaction periods and longer reduction periods, a stable catalyst activity could be achieved after several cycles. Once this status was attained, the catalyst was cooled to 453 K and data were taken between 453 and 498 K. The catalyst was then heated to 548 K, and data were taken between 548 and 498 K. By following this procedure, a check could be obtained for catalyst deactivation. In all cases the reaction rate measured at 498 K could be reproduced to within a few percent. It should be noted further that in all instances the conversion of CO was low, ranging from 0.02% at 453 K to 1.5% at 548 K.

RESULTS

Arrhenius plots for the rates of formation of C_1 through C_5 hydrocarbons over Ru_6/Al_2O_3 and Ru/SiO_2 are given in Figs. 1–5. The open points represent turnover numbers measured with H_2 and the solid points represent turnover numbers measured with D_2. The rates of formation of C_2 through C_4 paraffins and olefins have been shown separately in Figs. 2–4. Representation in this fashion was not possible, though, for the C_5 products since the resolution of the chromatographic peaks for olefins and paraffins was inadequate.

The data presented in Fig. 1 show that the production of CD_4 occurs approximately 1.5 times faster than CH_4 over Ru_6/Al_2O_3, both at 1 and 10 atm. At 10 atm

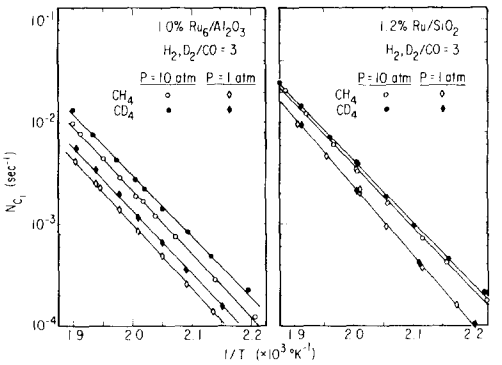

FIG. 1. Arrhenius plots for the formation of methane at 1 and 10 atm.

the production of CD_4 is also favored over Ru/SiO_2, but the magnitude of the inverse isotope effect is now 1.1. When the pressure is reduced to 1 atm, no isotope effect can be detected for this catalyst. It is noted further that the activation energy for both CH_4 and CD_4 lies between 27 and 28 kcal/mole, independent of the total pressure or catalyst composition.

Figures 2–5 show that an inverse isotope effect is also apparent for the production of C_2 through C_5 olefins and paraffins over the alumina-supported catalyst. The upward curvature of the Arrhenius plots for C_2D_6 and C_2H_6 can be explained in the following manner. For temperatures below about 493 K, olefins and paraffins are produced by parallel processes as suggested by the fact that the feed flow rate does not alter the olefin to paraffin ratio of the products.

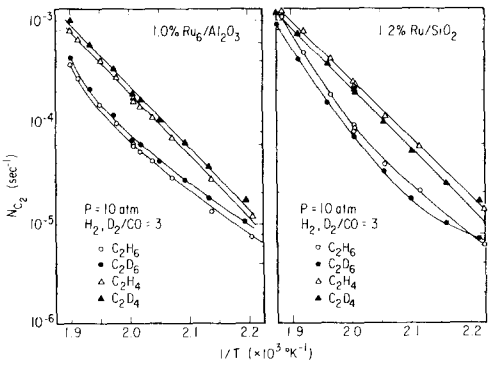

FIG. 2. Arrhenius plots for the formation of ethylene and ethane at 10 atm.

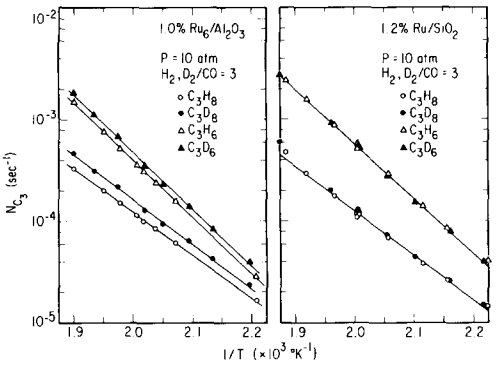

FIG. 3. Arrhenius plots for the formation of propylene and propane at 10 atm.

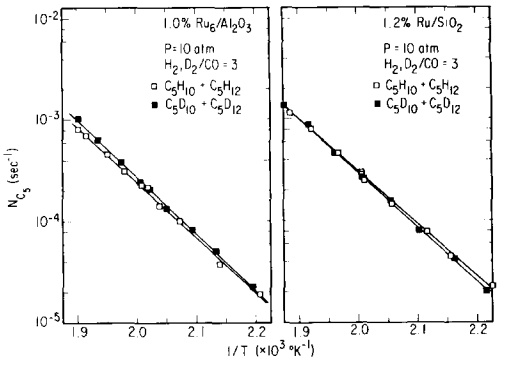

FIG. 5. Arrhenuis plots for the formation of pentene and pentane at 10 atm.

At higher temperatures, hydrogenation of the olefin takes place. The presence of this secondary reaction is confirmed by observing an increase in the olefin to paraffin ratio with increasing feed flow rate. When partial hydrogenation of the olefin product does occur, the Arrhenius plot curves upward, since the paraffin is now produced via two pathways.

Examination of the Arrhenius plots for C_2 through C_5 products formed over the Ru/SiO_2 catalyst shows that the isotope effects are significantly different from those observed using the alumina-supported catalyst. Normal isotope effects are seen for the C_2 and C_4 products but no significant isotope effect is found for the C_3 or C_5 products. Here again, the upward curvature in the Arrhenius plots for the C_2 through C_4 paraffins at higher temperatures can be ascribed to partial hydrogenation of the corresponding olefins.

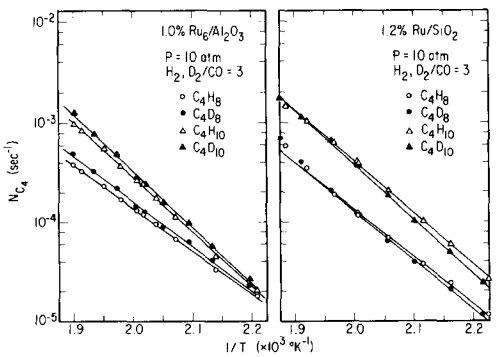

FIG. 4. Arrhenius plots for the formation of butene and butane at 10 atm.

Experiments identical to those shown in Figs. 2–5 were also carried out at 1 atm. The isotope effects for the alumina-supported catalyst were similar to those observed at 10 atm. Virtually no isotope effect was observed, though, for the silica-supported catalyst.

To determine whether the manner of preparation of the alumina-supported catalyst altered the nature or magnitude of the isotope effect, experiments were conducted with the Ru/Al_2O_3 catalyst prepared by reduction of $RuCl_3$. A comparison of the isotope effects for C_1 through C_5 hydrocarbons observed over the catalysts prepared from $Ru_6C(CO)_{17}$ and $RuCl_3$ is given in Table 1. It is seen that the isotope effects are virtually the same for the two catalysts. As a consequence, it seems appropriate to ascribe the observed isotope effects to the nature of the interactions between ruthenium and alumina rather than to the origin of the ruthenium.

The results presented in Table 1 indicate further that the magnitude of the isotope effect declines as the number of carbon atoms in the product increases. This trend is shown even more clearly in Fig. 6. Quite interestingly, for $n > 5$ the isotope effect becomes less than unity, indicating a slightly faster product formation rate with H_2 than with D_2.

TABLE 1

Comparison of the H_2/D_2 Isotope Effects for 1.0% Ru_6/Al_2O_3 and 3.0% Ru/Al_2O_3

	455 K		475 K		500 K	
	Ru_6/Al_2O_3	Ru/Al_2O_3	Ru_6/Al_2O_3	Ru/Al_2O_3	Ru_6/Al_2O_3	Ru/Al_2O_3
$N_{C_1}{}^D/N_{C_1}{}^H$	1.57	1.61	1.49	1.56	1.40	1.52
$N_{C_2}{}^D/N_{C_2}{}^H$	1.22	1.18	1.19	1.16	1.16	1.14
$N_{C_3}{}^D/N_{C_3}{}^H$	1.17	1.19	1.19	1.21	1.23	1.22
$N_{C_4}{}^D/N_{C_4}{}^H$	1.08	1.08	1.12	1.13	1.15	1.18
$N_{C_5}{}^D/N_{C_5}{}^H$	1.05	1.05	1.07	1.08	1.12	1.12

The effects of temperature on the olefin to paraffin ratio are shown in Figs. 7–9. For each catalyst, the ratio is observed to pass through a maximum with increasing temperature. The position of the maximum defines the temperature above which hydrogenation of the olefin becomes significant. For all three products the olefin to paraffin ratio is high when the silica-supported catalyst is used, but the temperature at which olefin hydrogenation becomes significant is higher for the alumina-supported catalyst. While the use of D_2 instead of H_2 does not influence the general characteristics of the olefin to paraffin ratio dependence on temperature, a number of subtle effects are apparent. For the alumina-supported catalyst, there is virtually no isotope effect on the olefin to paraffin ratios for C_2 and C_4 products. However, the ratio of propylene to propane is definitely higher when H_2 rather than D_2 is present in the feed. For the silica-supported catalyst, no isotope effect is detectable for the C_2 products at temperatures below 500 K. Above this temperature, though, the ethylene to ethane ratio is higher in the presence of D_2. By contrast, the olefin to paraffin ratios for the C_3 and C_4 products are higher in the presence of H_2 over the whole temperature range. The olefin to paraffin ratio was also examined for the data obtained at 1 atm. In this case the olefin to paraffin ratios were approximately threefold higher than those shown in Figs. 7–9 and higher values were obtained with H_2 than with D_2 for all three products over both catalyst.

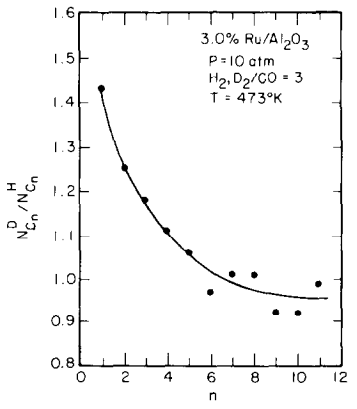

FIG. 6. Dependence of the isotope effect on the number of carbon atoms in the product.

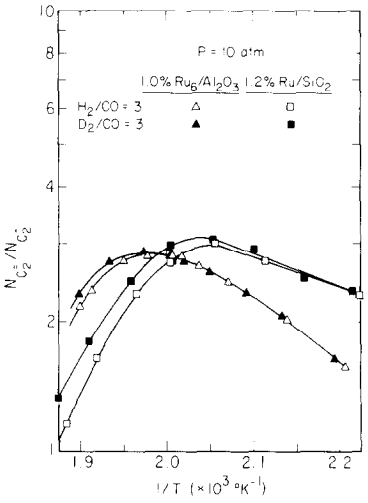

FIG. 7. Dependence of the olefin to paraffin ratio for C_2 products on the inverse temperature.

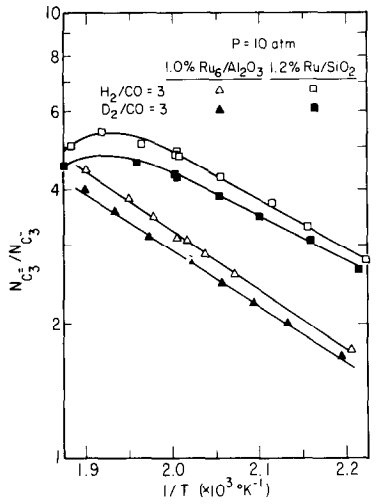

FIG. 8. Dependence of the olefin to paraffin ratio for C_3 products on the inverse temperature.

DISCUSSION

The data presented here clearly show that an inverse isotope effect can be observed for the formation of CH_4 over Ru catalysts. The magnitude of the effect is 1.6–1.4 for the alumina-supported catalysts, both at 1 and 10 atm. For silica-supported Ru the effect is 1.1 at 10 atm but drops to 1.0 at 1 atm. These results contradict the conclusion of Dalla Betta and Shelef (*21*) that there is no isotope effect for methane formation over Ru. Since the weight loading and dispersion of the catalyst used by Dalla Betta and Shelef were similar to that of the Ru_6/Al_2O_3 catalyst used in this work, it is difficult to understand why these authors did not observe an isotope effect. One possibility may be that an insufficient amount of data were taken, particularly with D_2. The present results also differ from those obtained by McKee (*20*). It should be noted, though, that comparison in this case may not be appropriate since McKee's studies were conducted with Ru powder at much lower pressures (60 Torr CO and 60 Torr H_2) and temperatures (298 to 423 K) than those used here. Furthermore, as was noted by Dalla Betta and Shelef (*21*), the analytical procedure used by McKee may not have been free of error. Products were detected by a mass spectrometer connected to the reaction chamber by a molecular leak. Since this method of sampling can give rise to different sensitivities for CH_4 and CD_4, and since calibration of the mass spectrometer was not discussed, it is not possible to know whether the reported results are accurate.

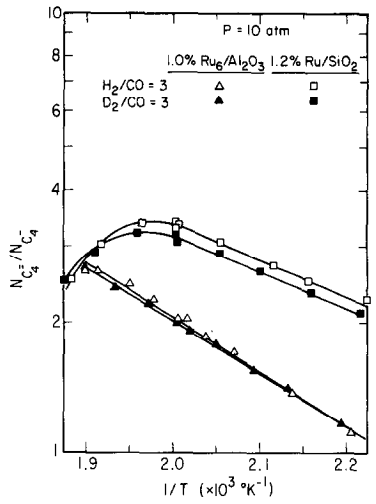

FIG. 9. Dependence of the olefin to paraffin ratio for C_4 products on the inverse temperature.

An interpretation of the isotope effects observed in the present study can be developed by consideration of the following reaction network:

1. $CO + S \rightleftarrows CO_s$
2. $CO_s + S \rightleftarrows C_s + O_s$
3. $H_2 + 2S \rightleftarrows 2H_s$
4. $H_2 + O_s \rightleftarrows H_2O + S$
5. $C_s + H_s \rightleftarrows CH_s + S$
6. $CH_s + H_s \rightleftarrows CH_{2s} + S$
7. $CH_{2s} + H_s \rightleftarrows CH_{3s} + S$
8. $CH_{3s} + H_s \rightarrow CH_4 + 2S$
9. $CH_{3s} + CH_{2s} \rightarrow C_2H_{5s} + S$
10. $C_2H_{5s} + S \rightarrow C_2H_4 + H_s + S$
11. $C_2H_{5s} + H_s \rightarrow C_2H_6 + 2S$
12. $C_2H_{5s} + CH_{2s} \rightarrow C_3H_{7s} + S$

etc.

This mechanism is supported by a significant number of recent investigations (*1–15*) and has been discussed in detail by

Bell (*27*). As a result, no attempts will be made here to justify the elementary steps included.

Overall rate expressions for the formation of methane can be derived from the proposed scheme provided a number of simplifying assumptions are invoked. The first is that the Ru surface is nearly saturated by adsorbed CO. This assumption is supported by *in situ* infrared observations carried out both at low and high pressure (*7, 26, 28, 29*). The second assumption is that water is the primary product through which oxygen is removed from the catalyst surface. Here, too, the assumption is substantiated by experimental evidence (*7, 26*). The third assumption is that all of the steps indicated as being reversible are, in fact, at equilibrium. No substantiation of this assumption is currently possible.

Two limiting forms can be obtained for the kinetics of methane formation, depending upon whether methanation or the synthesis of higher molecular weight hydrocarbons is dominant (*26, 27*). In the former case, the rate of methane formation is given by

$$N_{C_1} = k_e P_{H_2}^{1.5}/P_{CO} \tag{1}$$

$$k_e = \frac{K_3}{K_1}(k_4 k_8 K_5 K_6 K_7)^{1/2} \tag{2}$$

where k_i and K_i are the rate coefficient and equilibrium constant, respectively, for the ith elementary reaction. In the latter case, the rate is given by

$$N_{C_1} = k_e P_{H_2}^{1.5}/P_{CO}^{1.33} \tag{3}$$

$$k_e = k_8\left[\frac{k_4 K_2 K_3^{3.5} K_5 K_6 K_7^2(1-\alpha)}{k_p K_1^4}\right]^{1/3} \tag{4}$$

where k_p is the rate coefficient for the addition of CH_2 groups to adsorbed alkyls (i.e., reactions 9, 12, etc.) and α is the probability of chain propagation (*30*). With the exception of studies conducted at pressures of 1 atm or less, using H_2 to CO ratios greater than three, neither of the limiting assumptions is strictly valid. However, recent experimental studies by Kellner and Bell (*26*) have shown that for pressures between 1 and 10 atm and H_2/CO ratios between 1 and 3 the kinetics of methane formation can be described empirically by the expression $N_{C_1} = k_e P_{H_2}^{1.4}/P_{CO}$, in good agreement with Eq. (1).

The forms of Eqs. (1) and (3) indicate that the effective rate coefficient for methane synthesis is a complex product of rate coefficients and equilibrium constants. As a consequence, the observed isotope effect must result from the combination of kinetic and equilibrium isotope effects, as suggested by Wilson (*23*). To pursue the influence of these two effects further, it is useful to recall that rate coefficients and equilibrium constants can be expressed in the formalism of statistical mechanics (*31*). Thus,

$$k = \frac{kT}{h}\frac{q^{\ddagger}}{\prod_i q_r^{\nu_i}} \tag{5}$$

$$K = \frac{\prod_j q_p^{\nu_j}}{\prod_i q_r^{\nu_i}} \tag{6}$$

where (kT/h) is a frequency factor; q_r, q_p, and $q^{\ddagger}$ are the partition functions for reactants, products, and transition state complexes; and ν_i and ν_j are the stoichiometric coefficients for reactant i and product j. Changes in the magnitudes of k and K due to isotopic substitution result from the influences of molecular mass on the molecular partition functions. In most instances, the largest portion of the isotope effect arises from changes in the ground state vibrational frequencies.

Ozaki (*32*) has noted that the differences in the ground state vibrational frequencies of deuterated and hydrogenated species usually lead to the conclusion that the equilibrium constant for addition of deuterium to an adsorbed species is larger than that for the addition of hydrogen. An example of

this generalization which is relevant to the present discussion has been reported recently by Calvert *et al.* (*33*). In this work it was shown that deuterium is preferentially incorporated into methyl and methylene ligands present in triosmium complexes. The equilibrium constant for the reaction $Os_3(CO)_{10}CH_2D_2 \rightleftarrows Os_3(CO)_{10}CD_2H_2$ was determined to be 2.50 and that for the reaction $Os_3(CO)_{10}(CH_2D)D \rightleftarrows Os_3(CO)_{10}(CD_2H)H$ was found to be 1.74. Based on this evidence, one would suspect that the product $K_5K_6K_7$, appearing in Eqs. (1) and (3), should be significantly larger when D_2 is involved in steps 5 through 7 rather than H_2.

The equilibrium isotope effect for $H_2(D_2)$ chemisorption, reaction (3), can be examined explicitly. If it is assumed that the adsorbed atoms are immobile but have three degrees of vibrational freedom, then it readily be shown that

$$\frac{K_3^{D}}{K_3^{H}} = \left(\frac{m_{H_2}}{m_{D_2}}\right)^{5/2} \exp\left\{\left[-2\sum_{i=1}^{3}(\nu_i^{D} - \nu_i^{H}) + (\nu_1^{D_2} - \nu_1^{H_2})\right] h/(2kT)\right\} \quad (7)$$

where m_{H_2} and m_{D_2} are the masses of H_2 and D_2, ν_i^{H} and ν_i^{D} are the vibrational frequencies for adsorbed H and D atoms, and $\nu_1^{H_2}$ and $\nu_1^{D_2}$ are the vibrational frequencies for gaseous H_2 and D_2. Evaluation of K_3^{D}/K_3^{H} using the values of the vibrational frequencies given in Table 2 shows that this ratio lies between 0.79 and 0.62 for temperatures between 453 and 543 K. It is significant to note that while $K_3^{D}/K_3^{H} < 1$ over the temperature range of interest in these studies, the argument of the exponential factor in Eq. (7) leads to the expectation that the heat of adsorption for D_2 on Ru should be 1.34 kcal/mole larger than that for H_2. These conclusions are consistent with experimental observations on Ni. By means of calorimetric measurements on a Ni film, Wedler *et al.* (*34*) determined that the heat of adsorption of D_2 was about 1 kcal/mole larger than that for H_2. The displacement of adsorbed H atoms by D_2 and of adsorbed D atoms by H_2 on Ni catalysts was investigated by Gundry (*35*). His results showed that the apparent equilibrium constant for displacement, which is equivalent to K_3^{D}/K_3^{H}, varied from 2.4 at 178 K to near unity at 273 K. Based on this variation with temperature, it was estimated that the heat of adsorption of D_2 was 0.60 kcal/mole greater than that for H_2. The stronger adsorption of D_2 has also been confirmed by Wedler and Stanelmann (*36*) on a Ni film. Extrapolation of Gundry's results to the temperature levels used in this study would also lead to the conclusion that $K_3^{D}/K_3^{H} < 1$.

The kinetic isotope effect for reactions involving the addition of hydrogen has also been considered by Ozaki (*32*). Here again, he concludes that differences in the vibrational frequencies of deuterated and hydrogenated species are the primary origin of the effect and that in most cases $k_H > k_D$. For reactions involving a molecule of H_2 or D_2, and an adsorbed species (i.e., reaction 4), the ratio of masses arising from the transitional and rotational portions of the partition functions of H_2 and D_2 serve only to increase further the magnitude of the kinetic isotope effect.

Based upon the factors just considered, it is clear that the overall isotope effect on methane formation results from a complex combination of kinetic and equilibrium effects. Since the magnitude of these individ-

TABLE 2

Vibrational Frequencies for Molecular and Atomically Adsorbed H_2 and D_2

Species	Mode	Frequency (cm^{-1})[a]
H_2	ν(H–H)	4161
D_2	ν(D–D)	2993
M–H	ν(M–H)	2250–1700
	δ(M–H)[b]	800–600
M–D	ν(M–D)	1591–1202
	δ(M–D)[b]	566–424

[a] Taken from Nakamoto (*37*).
[b] Doubly degenerate.

ual effects cannot be predicted reliably, it is not possible to conclude whether the observed isotope effect is consistent with the structure of the effective rate coefficient appearing in Eqs. (1) and (3). What is evident, though, is that small changes in the isotope effects associated with individual elementary processes will alter the overall isotope effect. Such changes could arise from modifications of the metal dispersion and/or interaction with the support and might explain why the isotope effect is substantially smaller for the silica-supported catalyst than for either of the alumina-supported catalysts.

The data presented in Fig. 6 show that the magnitude of the inverse isotope decreases with increasing carbon number. This pattern can be understood in the following fashion. If it is assumed that the probability of chain propagation, α, is independent of chain length, n, then the rate of formation of hydrocarbons containing n atoms can be expressed as

$$N_{C_n} = (k_{to}\theta_v + k_{tp}\theta_H)\alpha^{n-1}\theta_{CH_3} \quad (8)$$

$$= \left(1 + \frac{k_{to}\theta_v}{k_{tp}\theta_H}\right)\alpha^{n-1}k_{tp}\theta_H\theta_{CH_3} \quad (9)$$

where k_{to} and k_{tp} are the rate coefficients for termination of chain growth by formation of olefins and paraffins (i.e., reactions 10 and 11), θ_v is the fraction of the catalyst surface which is vacant, and θ_H and θ_{CH_3} are the fractions of the surface covered by H atoms and CH_3 groups. The second term in the parantheses of Eq. (9) can be rewritten as

$$\frac{k_{to}\theta_v}{k_{tp}\theta_H} = \frac{k_{to}}{k_{tp}K_3^{1/2}P_{H_2}^{1/2}} \quad (10)$$

$$= \beta/P_{H_2}^{1/2}. \quad (11)$$

The magnitude of the isotope effect for any value of n can now be expressed by taking the ratio of the rate in the presence of D_2, $N_{C_n}^{D}$, to that in the presence of H_2, $N_{C_n}^{H}$. Combining Eqs. (9) and (11) with the expression $N_{C_1} = k_8\theta_H\theta_{CH_3}$, we obtain

$$\frac{N_{C_n}^{D}}{N_{C_n}^{H}} = \frac{k_{tp}^{D}}{k_{tp}^{H}}\frac{k_8^{H}}{k_8^{D}}\frac{(1 + \beta^{D}/P_{D_2}^{1/2})}{(1 + \beta^{H}/P_{H_2}^{1/2})}\left(\frac{\alpha^{D}}{\alpha^{H}}\right)^{n-1}\frac{N_{C_1}^{D}}{N_{C_1}^{H}}. \quad (12)$$

The form of Eq. (12) suggests that the isotope effect for any carbon number can be related to that observed for methane. To account for the decrease in $N_{C_n}^{D}/N_{C_n}^{H}$ with n it must be concluded that $\alpha^{D} < \alpha^{H}$. It is also noted that Eq. (12) predicts that for a sufficiently large value of n, $N_{C_n}^{D}/N_{C_n}^{H}$ could become less than one. While there is a considerable amount of scatter in the data for $n > 5$ shown in Fig. 6, it does appear that the isotope effect eventually becomes smaller than unity.

The influence of H_2 and D_2 on the olefin to paraffin ratio can also be understood in the context of the present discussion. The proposed reaction mechanism leads to the following expression for the olefin to paraffin ratio:

$$\frac{N_{C_n}^{=}}{N_{C_n}^{-}} = \frac{k_{to}}{k_{tp}K_3^{1/2}P_{H_2}^{1/2}} \quad (13)$$

$$= \beta/P_{H_2}^{1/2}.$$

This expression is found to be in good agreement with experimental data taken by Kellner and Bell (*26*) for temperatures below which olefin hydrogenation is not significant. The form of Eq. (13) again indicates that both kinetic and equilibrium isotope effects will influence the olefin to paraffin ratio. Since it has already been shown that $K_3^{D} < K_3^{H}$, the observation of a normal isotope effect on the olefin to paraffin ratio implies that $(k_{to}^{D}/k_{tp}^{D}) < (k_{to}^{D}/k_{tp}^{H})$ or alternatively that $(k_{to}^{D}/k_{tp}^{D}) > (k_{to}^{D}/k_{to}^{H})$.

CONCLUSIONS

The results of the present investigation have shown that an inverse isotope effect can be observed during the synthesis of CH_4 over silica- and alumina-supported Ru

catalysts, and that the magnitude of the effect is larger for alumina-supported catalysts.

Noticeable isotope effects have also been observed during the synthesis of C_2 through C_{11} olefins and paraffins. For C_2 through C_5 hydrocarbons, synthesis over an alumina-supported catalyst occurs more rapidly in the presence of D_2 rather than H_2, but the magnitude of the inverse isotope effect declines toward unity with increasing number of carbon atoms in the product. The synthesis of C_6 through C_{11} hydrocarbons appears to be favored by H_2, and, thus, a normal isotope effect is observed for these products.

The olefin to paraffin ratio of the products also depends on whether D_2 or H_2 is the reactant. Olefin formation is favored with H_2 over both silica- and alumina-supported catalysts.

The observed isotope effects can be rationalized on the basis of a mechanism proposed to describe the formation of CH_4 and higher molecular weight products. Rate expressions derived from this mechanism lead to the conclusion that the overall isotope effect results from a combination of the kinetic and equilibrium isotope associated with individual elementary steps. The proposed mechanism also provides explanations for the decline in the magnitude of the inverse isotope effect with increasing product carbon number and the higher olefin to paraffin ratio observed when using H_2.

ACKNOWLEDGMENT

This work was supported by the Division of Chemical Sciences, Office of Basic Energy Sciences, U.S. Department of Energy, under contract No. W-7405-ENG-48.

REFERENCES

1. Wentrcek, P. R., Wood, B. J., and Wise, H., *J. Catal.* **43,** 363 (1976).
2. Araki, M., and Ponec, V., *J. Catal.* **44,** 439 (1976).
3. Sexton, B. A., and Somorjai, G. A., *J. Catal.* **46,** 167 (1977).
4. Rabo, J. A., Risch, A. P., and Poutsma, M. L., *J. Catal.* **53,** 295 (1978)
5. Sachtler, J. W. A., Kool, J. M., and Ponec, V., *J. Catal.* **56,** 284 (1979).
6. Low, G. G., and Bell, A. T., *J. Catal.* **57,** 397 (1979).
7. Ekerdt, J. G., and Bell, A. T., *J. Catal.* **58,** 170 (1979).
8. McCarty, J. G., and Wise, H., *Chem. Phys. Lett.* **61,** 323 (1979).
9. Krebs, H. J., Bonzel, H. P., and Gafner, G., *Surf. Sci.* **88,** 269 (1979).
10. Goodman, D. W., and White, J.M., *Surf. Sci.* **90,** 201 (1979).
11. Bonzel, H. P., and Krebs, H. J., *Surf. Sci.* **91,** 499 (1980).
12. Bonzel, H. P., and Krebs, H. J., *ACS Div. Fuel Chem. Prepr.***25**(2), 8 (1980).
13. Kelley, R. D., Goodman, D. W., and Madey, T. E., *ACS Div. Fuel Chem. Prepr.* **25**(2), 43 (1980).
14. Biloen, P., Helle, J., and Sachtler, W. M. H., *J. Catal.* **58,** 95 (1979).
15. Ekerdt, J. G., and Bell, A. T., *J. Catal.* **62,** 19 (1980).
16. Luytens, L., and Jungers, J. C., *Bull. Soc. Chim. Belg.* **54,** 303 (1945).
17. Nicholai, J., Hont, M., and Jungers, J. C., *Bull. Soc. Chim. Belg.* **55,** 160 (1946).
18. Mori, T., Masuda, H., Imai, H., Miyamoto, A., and Murakami, Y., *Shokubai* **22,** 7 (1980).
19. Sakharov, M. M., and Dokukina, E. S., *Kinet. Katal.* **2,** 710 (1961).
20. McKee, D. W., *J. Catal.* **8,** 240 (1967).
21. Dalla Betta, R. A., and Shelef, M., *J. Catal.* **49,** 383 (1977).
22. Shelef, M., and Dalla Betta, R. A., *J. Catal.* **60,** 169 (1979).
23. Wilson, T. P., *J. Catal.* **60,** 167 (1979).
24. Kuznetsov, V. A., and Bell, A. T., *J. Catal.* **65,** 374 (1980).
25. Dalla Betta, R. A., *J. Phys. Chem.* **79,** 2519 (1975).
26. Kellner, C. S., and Bell, A. T., to be submitted.
27. Bell, A. T., *Catal. Rev. Sci. Eng.*, in press.
28. Dalla Betta, R. A., and Shelef, M., *J. Catal.* **48,** 111 (1977).
29. King, D. L., *J. Catal.* **77,** 61 (1980).
30. Madon, R., *J. Catal.* **57,** 183 (1979).
31. Laidler, K. J., "Chemical Kinetics," 2nd ed. McGraw-Hill, New York, 1965.
32. Ozaki, A., "Isotopic Studies of Heterogeneous Catalysis." Academic Press, New York, 1977.
33. Calvert, R. B., Shapley, J. R., Schultz, A. J.,

Williams, J. M., Suib, S. L., and Stucky, G. D., *J. Amer. Chem. Soc.* **100,** 6240 (1978).

34. Wedler, G., Bröker, F. J., Fisch, G., and Schroll, G., *Z. Phys. Chem. N.F.* **76,** 212, (1971).

35. Gundry, P. M., *Proc. 2nd Int. Congr. Catal.*, No. 51, 1083 (1960).

36. Wedler, G., and Stanelmann, G., *Ber. Bunsenges. Phys. Chem.* **75,** 1026 (1971).

37. Nakamoto, K., "Infrared Spectra of Inorganic and Coordination Compounds." 3rd ed. Wiley, New York, 1978.